

Bardia Yousefi<sup>1</sup>, Stefano Sfarra<sup>2,3</sup>, Clemente Ibarra Castanedo<sup>1</sup>, Xavier P. V. Maldague<sup>1</sup>

<sup>1</sup> Computer vision and systems laboratory, Department of Electrical and Computer Engineering, Laval University, 1065, av. de la Médecine, Québec, City (Québec) G1V 0A6, Canada

<sup>2</sup> University of L'Aquila - Las.E.R. Laboratory - Department of Industrial and Information Engineering and Economics (DIIE), Piazzale E. Pontieri no. 1, I-67100, Monteluco di Roio, Roio Poggio - L'Aquila (AQ), Italy, European Union

<sup>3</sup> Tomsk Polytechnic University, Lenin Av., 30, Tomsk 634050, Russia

## PROJECT DESCRIPTION

The goal of this research is the use of a covariance free decomposition approach called Candid Covariance-free Incremental Principal Component Thermography (CCIPCT). Here, there are several case studies investigated by CCIPCT for segmentation of the defects in artistic thermography and thermal non-destructive testing (NDT). It strives to consider the possibility of using CCIPCT in place of PCT.

## EXPERIMENTAL SETUP

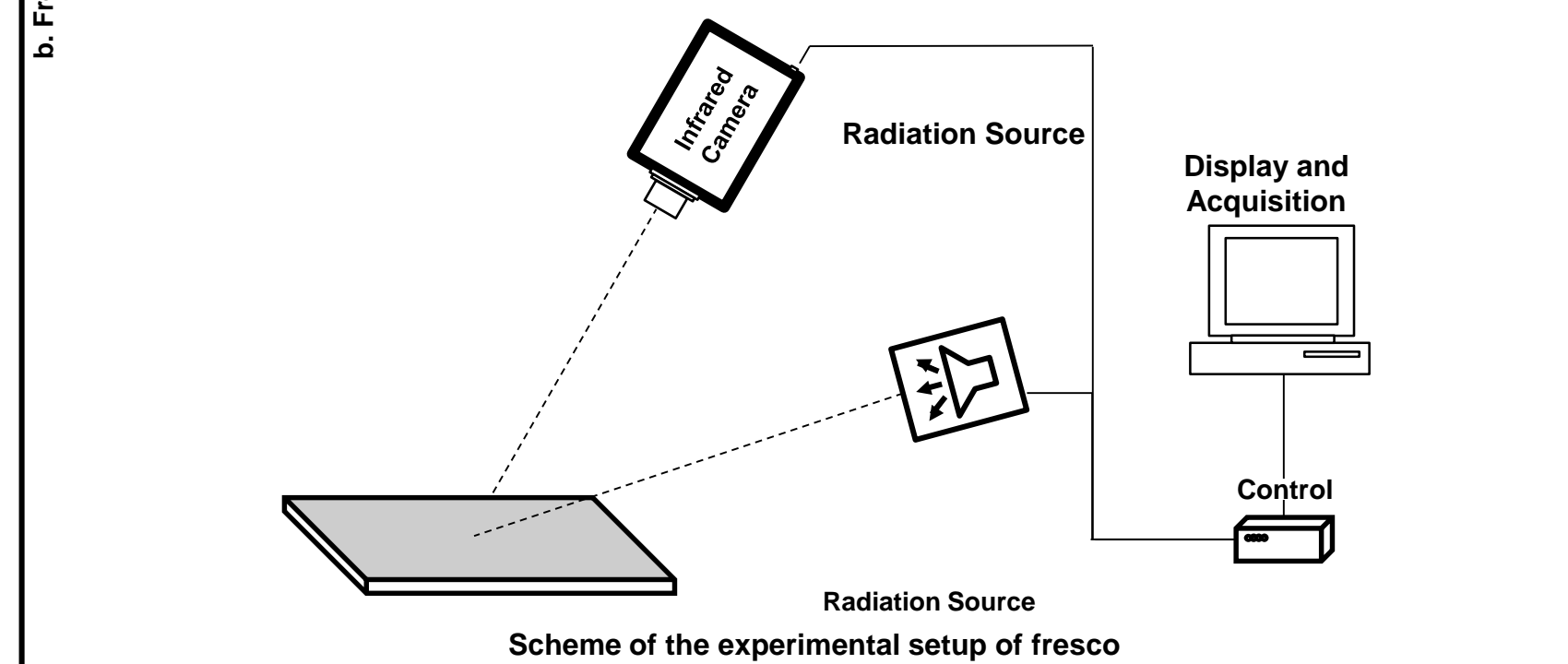
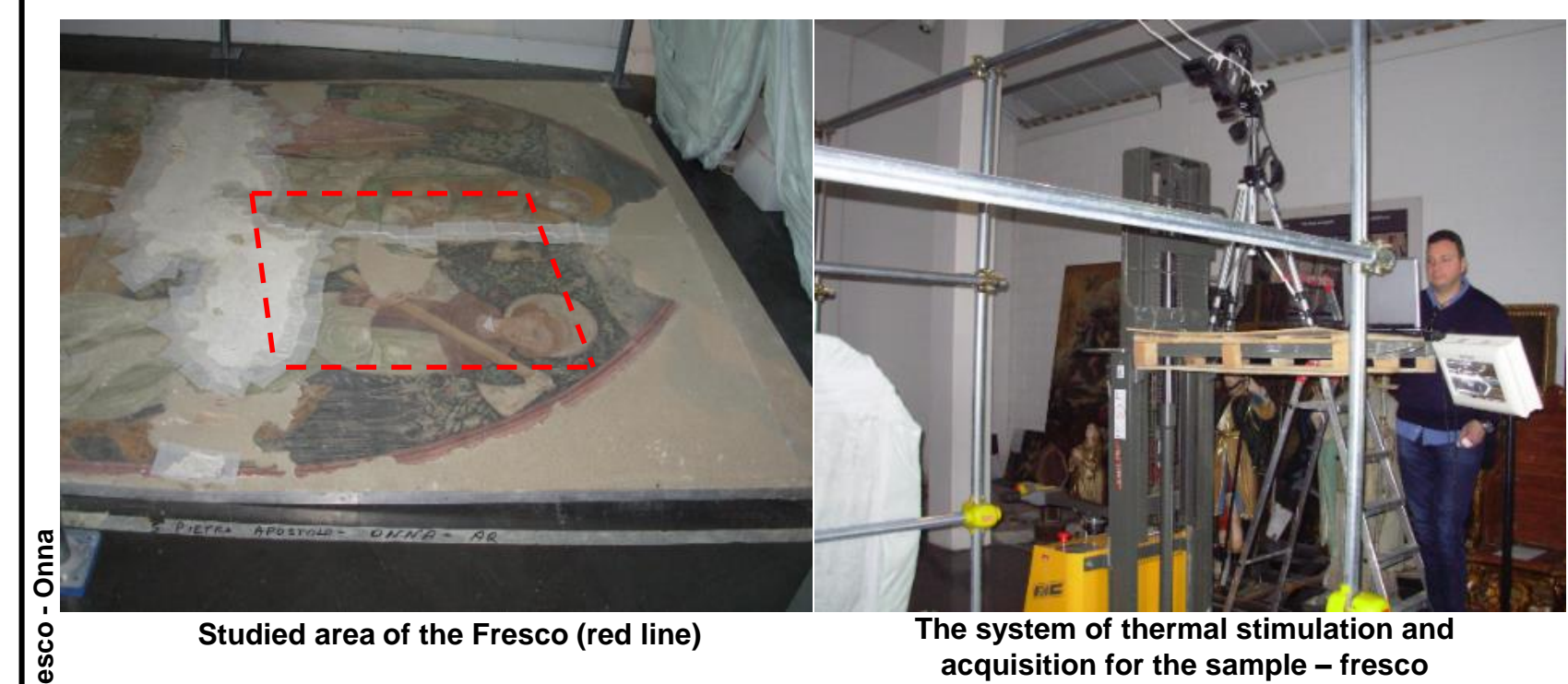
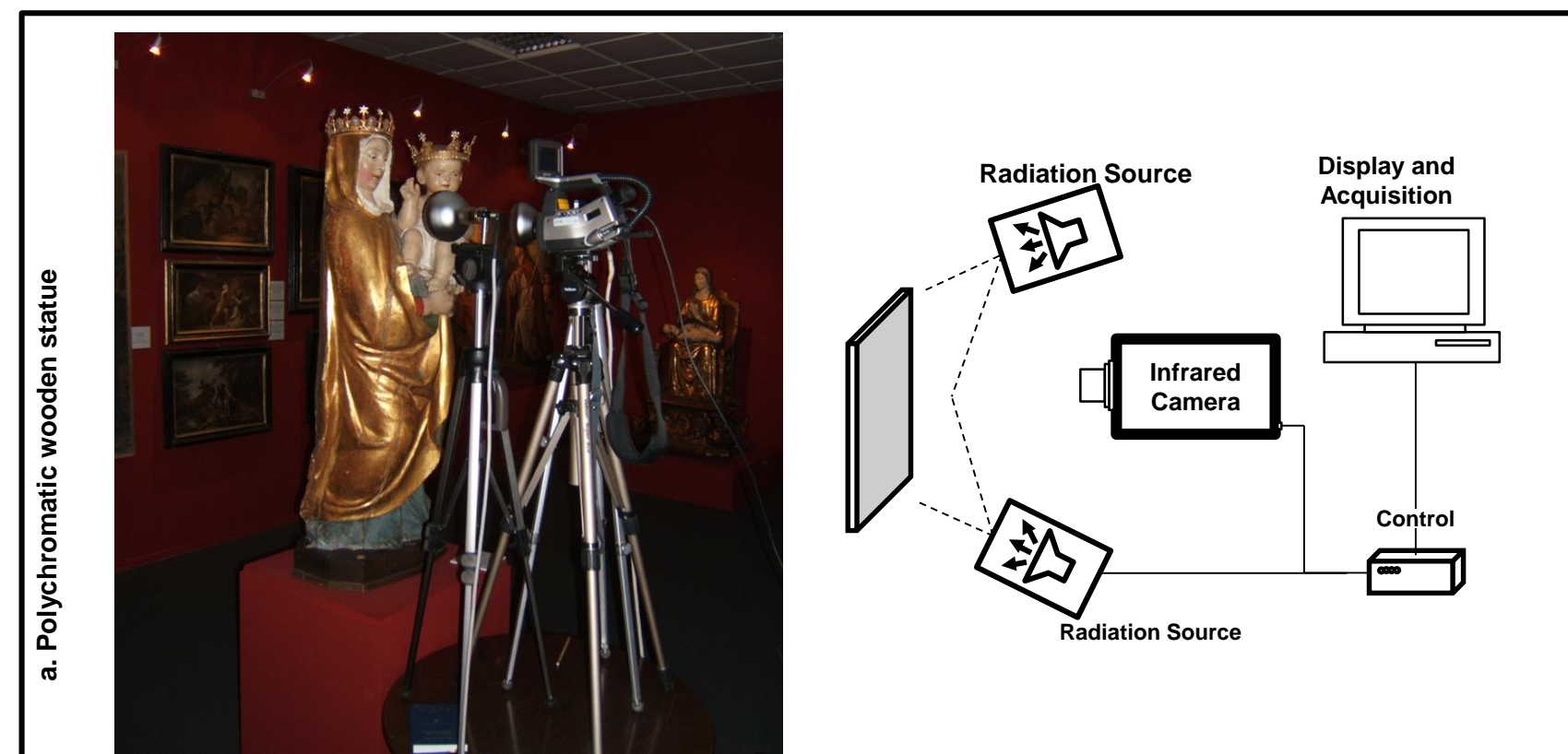
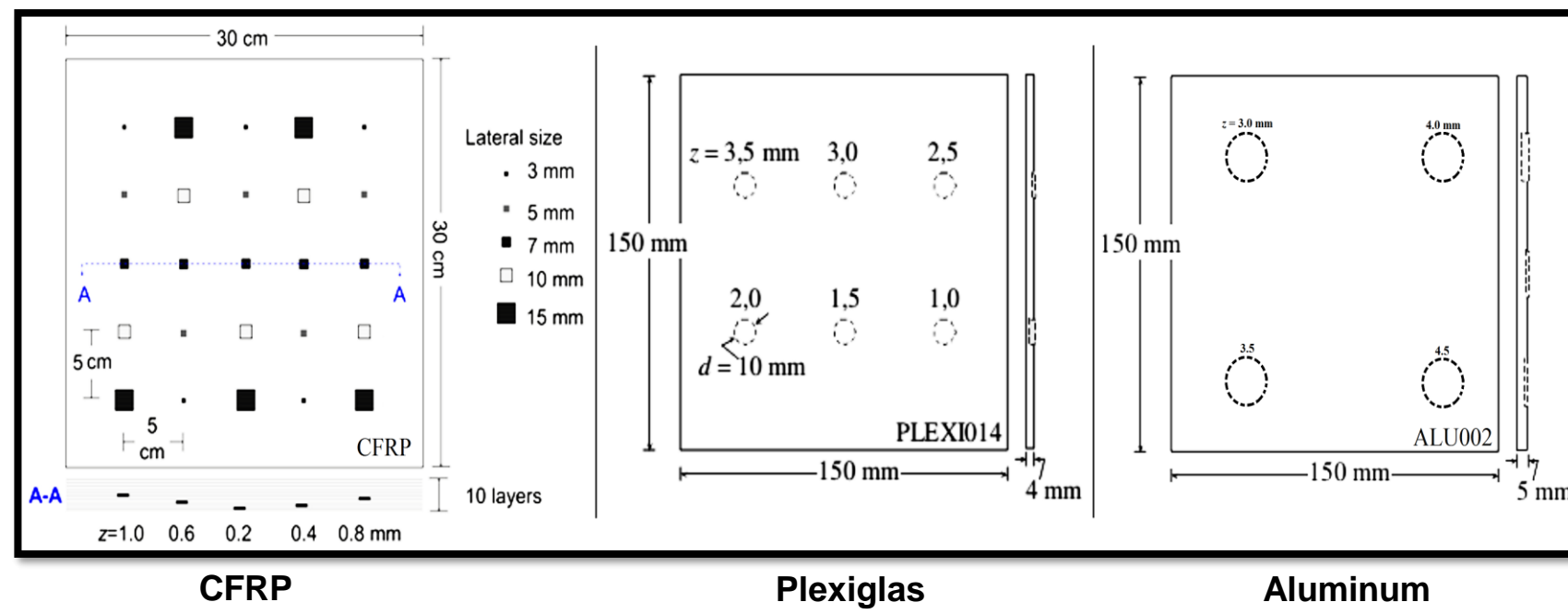
The inspection was conducted from the front side of the specimen CFRP (CFRP having the depths range from 0.2 to 1 mm, Plexiglas from 1 to 3.5 mm, and Aluminium from 3.5 to 4.5 mm). Two photographic flashes were used: Balcar FX 60, 5ms thermal pulse, 6.4 kJ/flash. The infrared camera was a mid-wave infrared (MWIR) cooled by lique nitrogen (320 \* 256 pixels). The sampling rate was 157 Hz, and a total of 1000 images were acquired. In the two other image sets, the condition were similar side of inspection photographic flashes and infrared camera but there were some minor changes in the tuning of acquisition parameters<sup>1</sup>.

### Polychromatic statue<sup>2</sup>

The infrared camera used was a long wave infrared camera (LWIR - 7.513 μm) having the spatial resolution of 240 \* 320 pixels. There were two radiation sources, i.e., two 250 W SICCATHERM E27 lamps that gave a wide radiation spectrum for thermography testing. During the test, the infrared thermography acquisition process was controlled using the spot function and the lamps were located far from the specimens (24cm) to provide an adequate heating up phase. The distance lamp - lamp was 40 cm, while the thermal camera was put at 46cm from the left cheek of the Child. The relative humidity(RH) was 47.5% and the emissivity value was set at 0.90. The six hundred thermograms were recorded during 180 seconds of heating and seven minutes of cooling (420 thermograms).

### Fresco - Onna<sup>2</sup>

In the experiment of the real fresco, the heating up phase during the inspection by infrared thermography (IRT) lasted 360 seconds. The camera was installed at 295cm from the sample surface, while 1 lamp (2kW) put at the distance of 235cm was used. In the early stage of the thermographic campaign, the ambient temperature recorded was 16.2 °C, while the relative humidity (RH) was equal to 40.1%. Also in this case, the emissivity value was set at 0.90, although the new technique applied minimize the emissivity variation due to the nature of the pigments. The cooling down phase lasted 780 seconds, and 1 thermogram per second was recorded during the entire inspection procedure. The experimental setup is shown in the figure b.

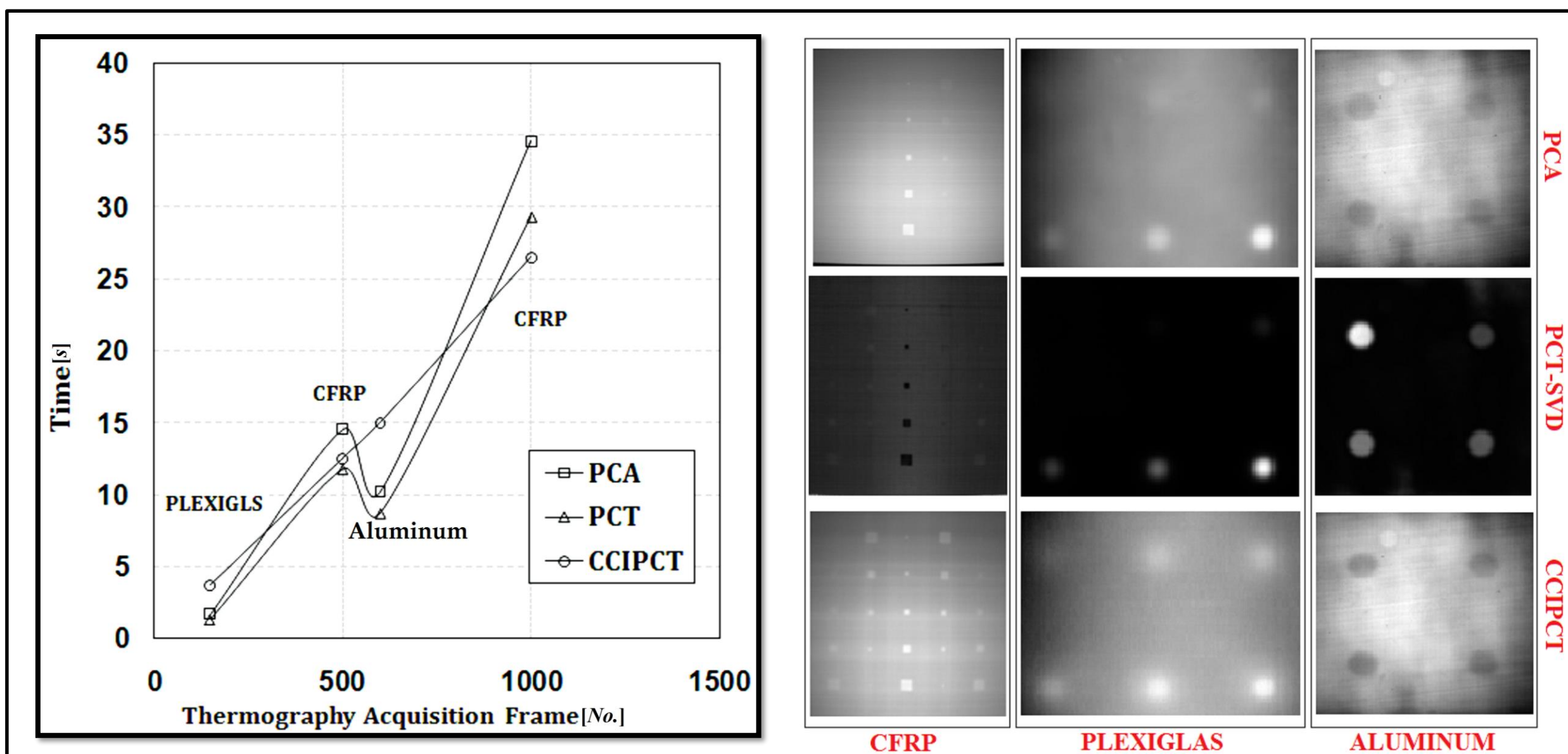


## CCIPCT

For calculating the CCIPCT, suppose that the data is zero mean,  $u = x - E[x]$ .  $x$  and  $E[x]$  are our input data and mean of input data, respectively. Then  $u(n)$  is zero mean data which even mean can be incrementally estimated. The general definition of eigenvalue and eigenvector problem formulates as follows:

$$E[u, u^T] v_i^* = \lambda_i^* v_i^*$$

where  $\lambda$  corresponds to eigenvalue diagonal matrix in descending order of the eigenvalues ( $\lambda_1^* \geq \lambda_2^* \geq \dots \geq \lambda_k^*$ ) and  $v$  is the matrix of the eigenvector of our data. It means the  $\lambda_i^*$  is the eigenvalue corresponding to the variance of  $v_i^* v_i^{*T}$  and shown by  $\hat{D}$  which is a diagonal matrix having  $1/\sqrt{\lambda_i^*}$ . The property of CCIPCT makes it more efficient as compare to PCT that is updating the  $D$  and  $V$  matrices for each sample. Updating CCIPCT ( $u_i$ ), as an observation set, requires an estimation of  $v_i$  ( $v_i(t-1) \rightarrow v_i(t)$ ) and update it for everytime along with projection of  $u_i(t) \rightarrow u_{i+1}(t)$ . It continues till coverage to the true components<sup>3,4</sup>.



Experimental analysis regarding aluminum, Plexiglas and CFRP with two different sets of acquisition video frame streams is shown to prove the capability of the proposed approach for high dimensional video streams. Specimen applying PCA-Covariance matrix (presented in first row), PCT-SVD (second row) and CCIPCT technique (shown in the third row). CCIPCT showed lower computational load while the number of the frames increase. Note that with fewer acquisition frames other techniques such as PCT increase have a reasonable computational expense however the ability to be an on-line process will not be possible. Experimental analysis for CFRP, Plexiglas, and aluminum specimens applying PCT (one uses optimized PCA code of MATLAB (first row), PCT (second row) and CCIPCT approach (third row). The first Eigen-image using of each method are presented. The First-CCIPCT can be more considerable representative of the defects than other methods. However, the other Eigen-images might provide more details.

We thank NSERC(Natural Sciences and Engineering Research Council of Canada). This research is conducted under Canada research chair in Infrared and Thermography.

## RESULTS

The results of all specimens are shown in below mentioned figure for PC1 and PC2 for PCA, PCT, CCIPCT. It represents the great advantage and drawback of CCIPCT in representing the defects.

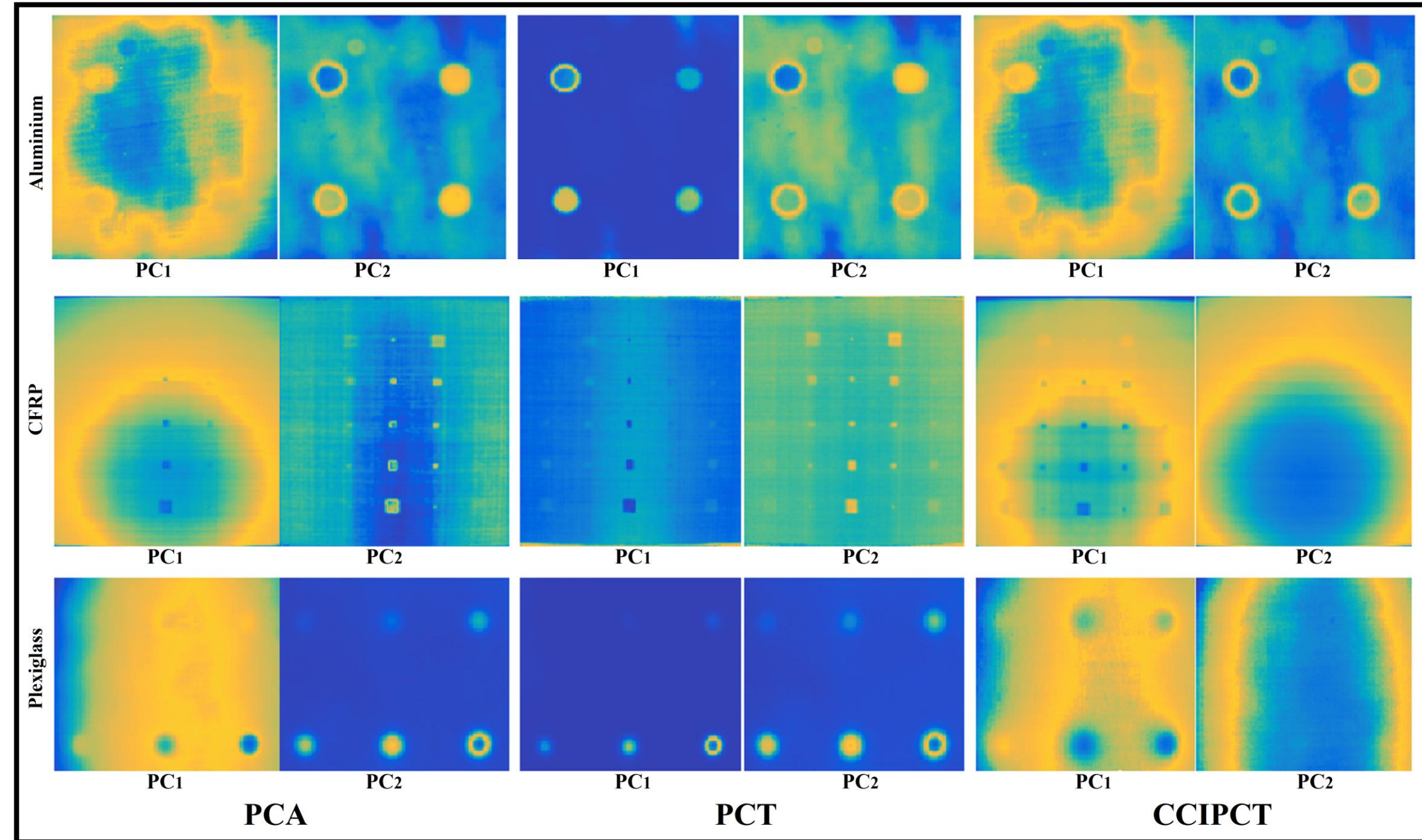
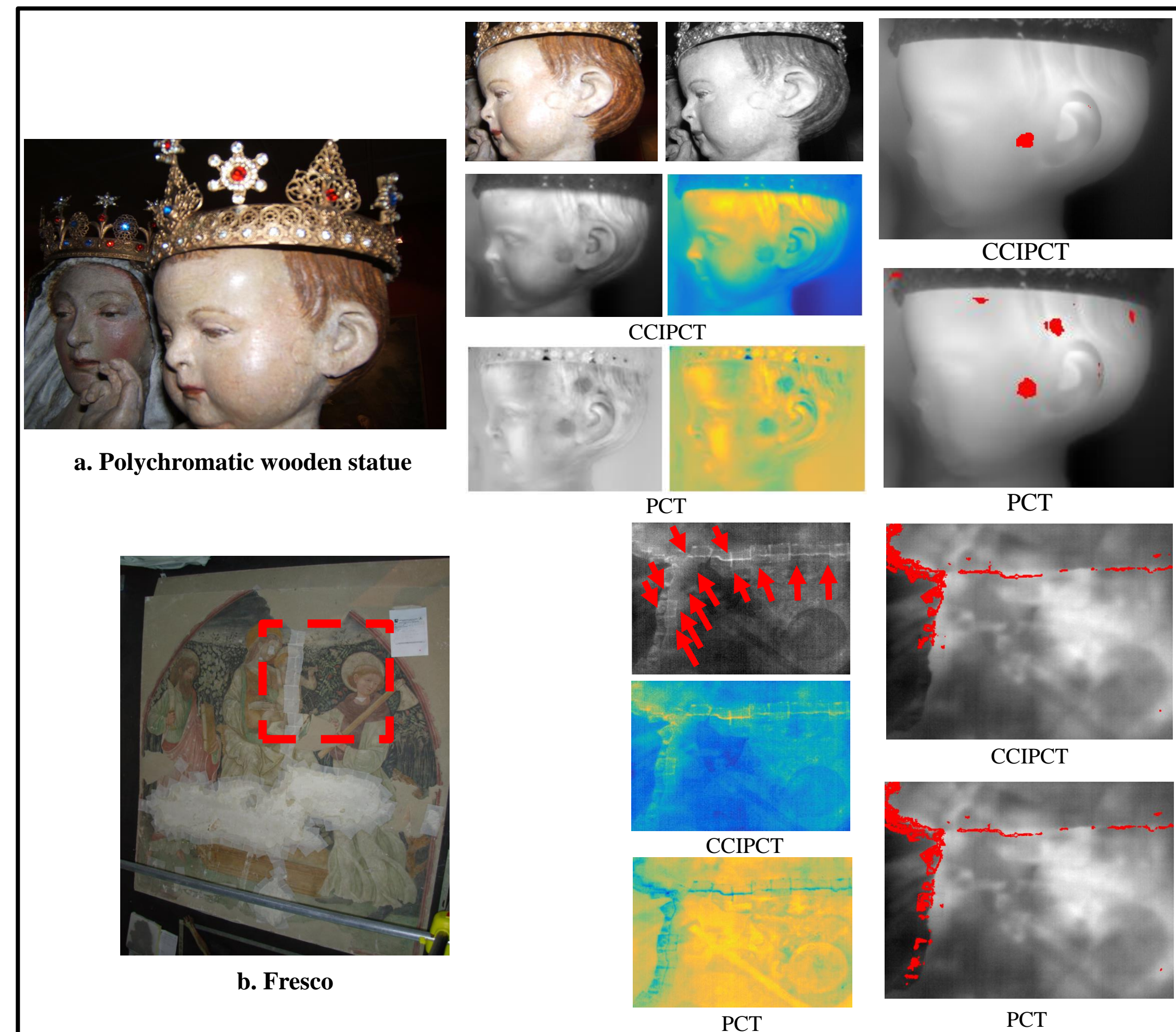


Figure below depicts the results of CCIPCT and PCT for polychromatic wooden statue and Fresco. Also the detected defects are depicted in each section which is represented the ultimate purpose of such techniques.



## SUMMARY

Thermal and infrared imagery creates considerable developments in Non-Destructive Testing (NDT) and many other areas. In the arts and archaeology field, infrared technology provides significant contributions in term of finding defects of possible impaired regions. This has been done through a wide range of different thermographic experiments and infrared methods.

Here, a thermography method for specimens inspection is addressed by applying a technique for computation of eigen-decomposition which refers as Candid Covariance-Free Incremental Principal Component Thermography (CCIPCT). The proposed approach uses a shorter computational alternative to estimate covariance matrix and Singular Value Decomposition(SVD) to obtain the result of Principal Component Thermography(PCT) and ultimately segments the defects in the specimens applying color based K-medoids clustering approach. The problem of computational expenses for high-dimensional thermal image acquisition is also investigated. Three types of specimens (CFRP, Plexiglas and Aluminum) plus two artistic objects as specimens (a polychromatic wooden statue and a fresco) have been used for comparative benchmarking. The results conclusively indicate the promising performance and demonstrated a confirmation for the outlined properties.

## References

- [1] C. Ibarra-Castanedo, X. P. Maldague, *Defect depth retrieval from pulsed phase thermographic data on plexiglas and aluminum samples*, in: Defense and Security, International Society for Optics and Photonics, 2004, pp. 370-378.
- [2] Sfarra, S., Ibarra-Castanedo, C., Paoletti, D., and Maldague, X., *Infrared vision inspection of cultural heritage objects from the city of laquila, Italy and its surroundings*, Materials Evaluation 71(5) (2013).
- [3] D. Peng, Z. Yi, W. Luo, *Convergence analysis of a simple minor component analysis algorithm*, Neural Networks 20 (7) (2007) 842-850.
- [4] J. Weng, Y. Zhang, W.-S. Hwang, *Candid covariance-free incremental principal component analysis*, IEEE Transactions on Pattern Analysis and Machine Intelligence 25 (8) (2003) 1034-1040.

